Journal of Nematology 47(2):105–115. 2015.
© The Society of Nematologists 2015.

Diplogasteroides asiaticus n. sp. is Associated with *Monochamus alternatus* in Japan

Natsumi Kanzaki,[1] Gavin C. Woodruff,[1] Mitsuteru Akiba,[1] and Noritoshi Maehara[2]

Abstract: Diplogasteroides asiaticus n. sp. is described and illustrated, and its molecular profile and phylogenetic status within the family Diplogastridae are inferred. Morphologically, the new species is characterized by its stomatal structure, a tube-like stoma with three small, rod-like dorsal teeth and two subventral ridges; a spicule clearly ventrally bent at 1/3 from the anterior end; a gubernaculum with a rounded anterior end and sharply pointed distal end in lateral view; nine pairs of genital papillae with an arrangement of <v1, (v2, v3d), C, v4, ad, ph, (v5, v6, v7), pd>; a short tail spike in males; and a well-developed *receptaculum seminis*, i.e., the antiparallel blind sacs of the uteri beyond the vulva region and elongated conical tail in females. This new species is morphologically similar to *D. haslacheri*, but it can be distinguished by the morphology of the somewhat shorter tail in females. *D. asiaticus* n. sp. shares high sequence conservation with *D. andrassyi* as there is only one base pair difference in the nearly full-length 18S rDNA and seven base pair differences in the D2-D3 expansion segments of the 28S rDNA. Despite this sequence conservation, the species status of *D. asiaticus* n. sp. was confirmed using the biological species concept, as *D. asiaticus* n. sp. and *D. andrassyi* failed to generate viable F_2 progeny in hybridization tests.

Key words: Diplogasteroides asiaticus n. sp., Japan, *Monochamus alternatus*, morphology, phylogeny, *Pinus densiflora*, taxonomy.

The genus *Diplogasteroides* de Man, 1912 is currently characterized by its tube-like stoma with three small, rod-like dorsal teeth and nine pairs of genital papillae in males with an arrangement in the general diplogastrid pattern, while some other characters are divergent among the species, e.g., the genus contains monodelphic and didelphic species (Sudhaus and Fürst von Lieven, 2003). The genus is considered a possible paraphyletic taxon, because there is no clear genus-specific apomorphy, i.e., many of the generic characters overlap with other diplogastrid genera (Sudhaus and Fürst von Lieven, 2003). Molecular phylogenetic analyses revealed paraphyly, where three didelphic species are separated into two clearly different clades: *Diplogasteroides* sp. RS5444 + *D. magnus* Völk, 1950 is separated from *D. andrassyi* Kanzaki, Tanaka, Hirooka, and Maehara, 2013 within the family Diplogastridae Micoletzky, 1922 (Kanzaki et al., 2013). Furthermore, Susoy et al. (2015) and Kanzaki and Giblin-Davis (2015) suggested that monodelphic species form a well-supported clade, and a genus, *Fuchsnema* Andrássy, 1984 could be resurrected for a home of several monodelphic species. Therefore, to organize the genus taxonomically, more specimens with detailed morphological descriptions and molecular markers are necessary.

Despite the current situation, we consider that a new species description for the genus using detailed morphological information is worthwhile for the accumulation of information for a future generic revision. A new species that shares high sequence and morphological similarity to a previously described species, *D. andrassyi*, is described and illustrated as *D. asiaticus* n. sp. Furthermore, the molecular sequences of the nearly full-length 18S (small subunit) ribosomal RNA gene (SSU) and the D2-D3 expansion segment of the 28S (large subunit) ribosomal RNA gene (D2-D3 LSU) from the new species are ascribed as species-specific molecular markers.

Materials and Methods

Nematode isolates: Several dead logs of *Pinus densiflora* Sieb. and Zucc. were collected from the Chiyoda Experimental Station of the Forestry and Forest Products Research Institute (FFPRI), Kasumigaura, Ibaraki, Japan, in April 2013. The logs were kept in a wire-mesh cage at FFPRI. Adults of *Monochamus alternatus* Hope that emerged from June to July 2013, were collected and dissected to examine their nematode associates. The diplogastrid dauers isolated from male genitalia or female ovipositors of the beetles were transferred to a nematode growth medium (NGM) plate seeded with *Escherichia coli* strain OP50. The dauers molted to fourth-stage juveniles in a few days and developed into adults. Successfully propagated nematodes were subcultured occasionally on NGM-OP50 plates and kept as laboratory cultures.

Morphological observations: Cultured nematodes were used for morphological observations. Live materials picked directly from 1- to 2-wk-old cultures were used for drawings and micrographs. To observe the morphology in detail (e.g., stomatal morphology and the ventral view of the male tail), silicone grease and squashing methods (Kanzaki, 2013) were employed. The materials collected from a 10-d-old culture were killed by heat (60°C, 1 min) and fixed with triethanolamine formalin (TAF), processed using a glycerin–ethanol series using the modified

Received for publication January 13, 2015.
[1]Forest Pathology Laboratory, Forestry and Forest Products Research Institute (FFPRI), 1 Matsunosato, Tsukuba, Ibaraki, 305-8687 Japan.
[2]Tohoku Research Center, FFPRI, 92-25 Nabeyashiki, Shimo-Kuriyagawa, Morioka, Iwate, 020-0123 Japan.
We thank Noriko Shimoda and Atsuko Matsumoto, FFPRI for their assistance in nematode culturing and molecular sequencing, respectively.
This study was supported in part by the Grant-in-Aid for Scientific Research (Challenging Exploratory Research), 2012, no. 70435585 from the Japan Society for the Promotion of Science and Environment Research and Technology Development Fund (4-1401) from the Ministry of the Environment, Japan.
Natsumi Kanzaki and Gavin C. Woodruff contributed equally as co-senior authors.
Email: nkanzaki@affrc.go.jp
This paper was edited by Christine Griffin.

Seinhorst's methods (Minagawa and Mizukubo, 1994) and mounted in glycerin according to the methods of Maeseneer and d'Herde (Hooper, 1986). The mounted specimens were designated as type materials.

Molecular profiles and phylogeny: For molecular analysis, nematodes were transferred individually to 30 µl nematode digestion buffer (Kikuchi et al., 2009; Tanaka et al., 2012) and digested at 60°C for 20 min, then the crude DNA solution was used as the PCR template. DNA base sequences of partial ribosomal DNA (ca. 1.7-kb nearly full-length small subunit [SSU] and 0.7-kb D2-D3 expansion segment of the large subunit [D2-D3 LSU]) and 0.7-kb mitochondrial cytochrome oxidase subunit I (mtCOI) were determined for *D. asiaticus* n. sp. following the methods of Kanzaki and Futai (2002) and Ye et al. (2007).

The molecular phylogenetic status of *D. asiaticus* n. sp. was determined based on the SSU sequence using Bayesian analysis. The species (operational taxonomic units [OTU]) that were compared with *D. asiaticus* n. sp. were determined according to the results of a BLAST homology search (http://blast.ncbi.nlm.nih.gov/Blast.cgi) and the OTU used in a previous study of a species description of *D. andrassyi* (Kanzaki et al., 2013). The compared sequences were aligned using MAFFT (Katoh et al., 2002; available online at http://align.bmr.kyushu-u.ac.jp/mafft/software/) and the base substitution model was determined as GTR + I + G using MODELTEST version 3.7 (Posada and Crandall, 1998) under the Akaike information criterion (AIC) model selection criterion. The Akaike-supported model, log likelihood (lnL), the AIC values, proportion of invariable sites, gamma distribution shape parameters, and substitution rates were used in the analyses. Bayesian analysis was performed using MrBayes 3.2 (Huelsenbeck and Ronquist, 2001); four chains were run for 4×10^6 generations. Markov chains were sampled every 100 generations (Larget and Simon, 1999). Two independent runs were performed and after confirming the convergence of runs and discarding the first 2×10^6 generations as "burn in," the remaining topologies were used to generate a 50% majority-rule consensus tree.

Hybridization tests: Because the new species shares high sequence conservation with *D. andrassyi* (details described below), a hybridization experiment was conducted to confirm its species status. *D. andrassyi* strain NK303 (type strain, see Kanzaki et al., 2013) was used as the reference strain. Animals were maintained using standard *Caenorhabditis elegans* conditions (NGM plates seeded with *E. coli* strain OP50; Wood, 1988). Crosses were performed at 25°C. Each cross was performed with three females and six to eight males. Conspecific control crosses and reciprocal heterospecific crosses were performed. Sexually immature female juveniles were used to assure virginity. Crosses were monitored periodically for 10 d for the presence of progeny.

Results

Diplogasteroides asiaticus n. sp.
(Figs. 1–6)

Measurements: See Table 1.

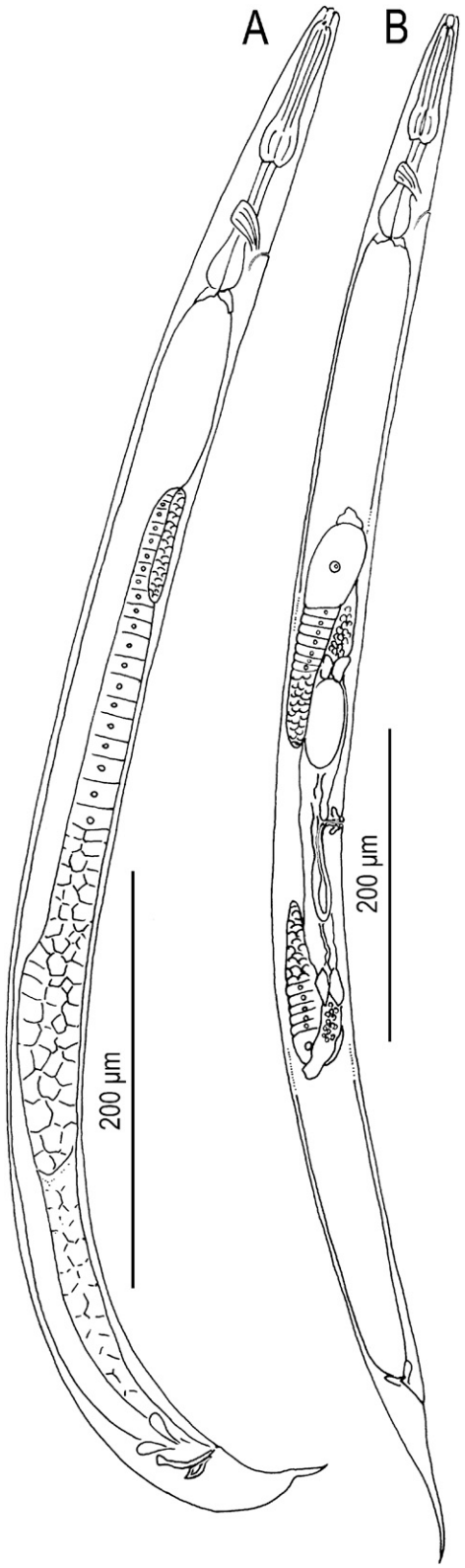

Fig. 1. *Diplogasteroides asiaticus* n. sp. A. Male. B. Female.

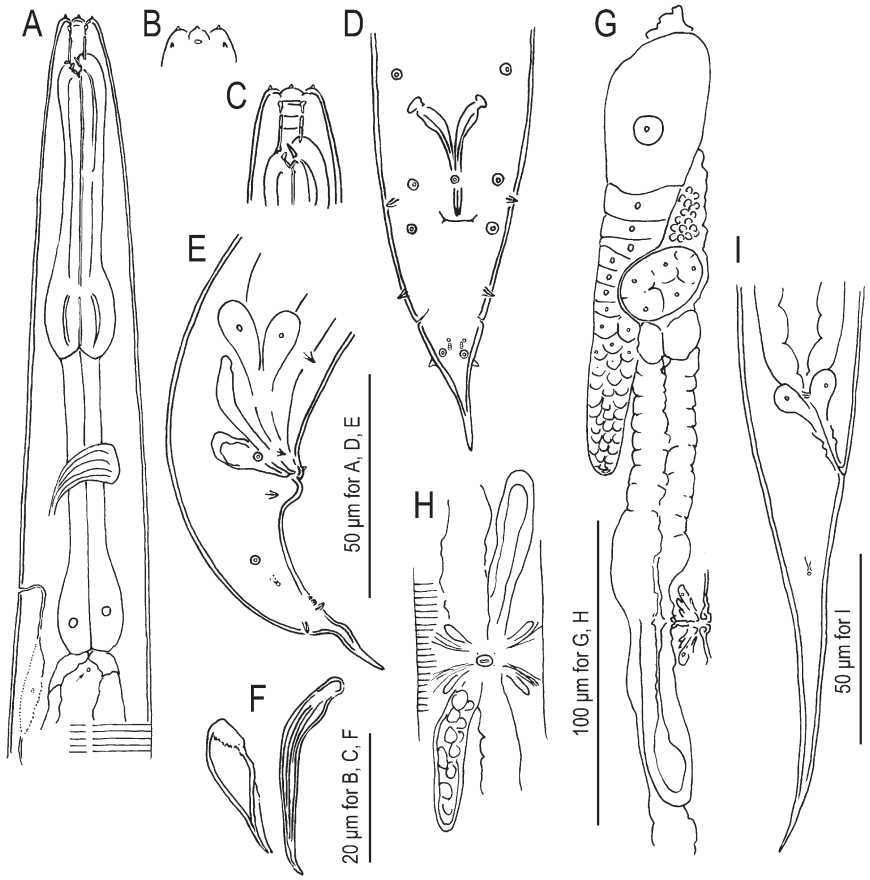

Fig. 2. *Diplogasteroides asiaticus* n. sp. A. Anterior part of the male in left lateral view. Deirid is suggested by an arrow. B. Anterior end of the male (surface). C. Left lateral view of the stoma. D. Ventral view of the male tail. E. Right lateral view of the male tail. F. Right lateral view of the spicule and gubernaculum. G. Right lateral view of the anterior female gonad. H. Ventral view of the female vulval region and annulations on body surface. I. Right lateral view of the female tail.

General: Moderate to slender nematode. Body cylindrical, anterior and posterior ends tapered. Cuticle moderate in thickness, weak annulation on the surface, striation not clearly observed. Lateral field composed of two lines, unclear, very weakly distinguished with lack of annulation. Lip region not offset, not clearly separated from the other parts of the body, weakly separated into six sectors; each sector possesses a setiform labial sensilla

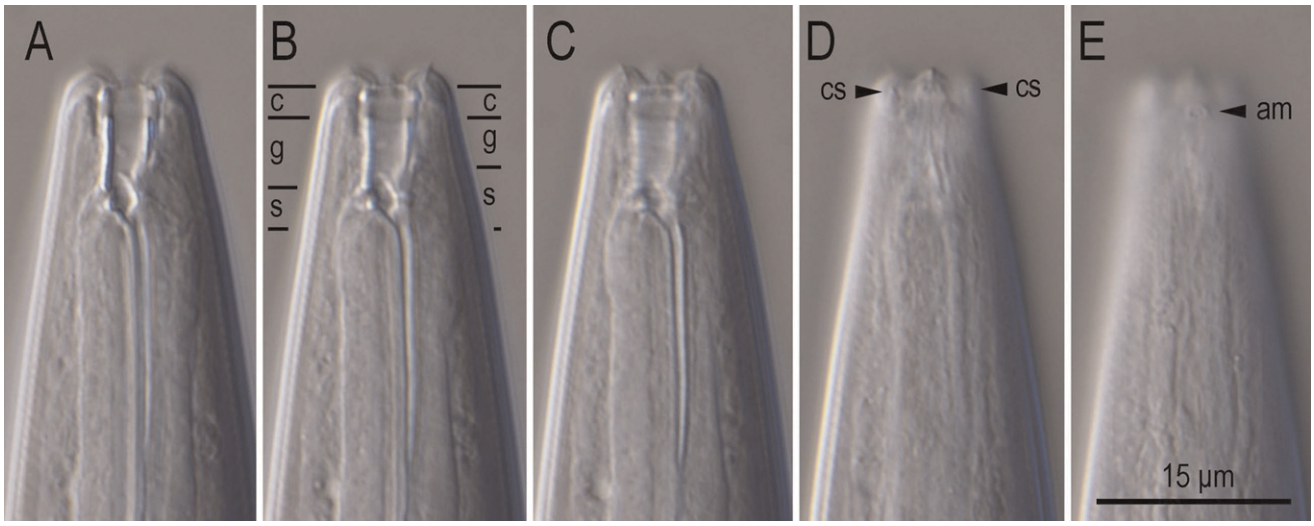

Fig. 3. Left lateral view of the male stomatal region of *Diplogasteroides asiaticus* n. sp. in different focal planes. Separation of the stomatal elements (c: cheilostom, g: gymnostom, s: stegostom) is shown in B. Cephalic sensilla (cs) and amphid (am) are shown in D and E, respectively.

Fig. 4. Left lateral view of the pharynx region of *Diplogasteroides asiaticus* n. sp. in different focal planes showing the nerve ring (nr) and excretory pore (ep).

and four extra sensilla, one on each dorsal and ventral sector, in males only. Small oval-shaped amphidial openings present at the lateral lip sectors at the level of the posterior end of the cheilostom. Deirid small, visible around the level of the basal bulb and cardia, clearly posterior to the excretory pore. Inner wall of the lip sectors a little elongate and forming a small flap covering the stomatal opening. Stoma tube-like, separated into three sections: cheilostom, gymnostom, and stegostom. Cheilostom short, with thick and ring-like anterior part and thin and short tube-like posterior part; anterior part is wider than posterior part, creating a refractal dot-like appearance in light microscopic views. Gymnostom well-cuticularized, tube-like, twice as long as the cheilostom, dorsal side clearly shorter than ventral side, possessing weak annulations, i.e., transverse striations, on the whole part. Gymnostom is separated into two subsections, each hypothesized to be associated with arcade syncytia: dorsal and ventral walls of the anterior subsection equal in length, i.e., forming a short tube, a little thicker than the posterior subsection; stomatal wall of the posterior subsection thinner than the anterior subsection, ventral wall twice as long as the dorsal wall. Stegostom separated into subsections, pro-meso-, meta-, and telostegostom. Pro-mesostegostom not cuticularized, anisotopic and ansiomorphic; dorsal wall expanded internally, i.e., mound-like expansion; ventral wall not conspicuous. Metastegostom bearing three small dorsal teeth; the central one is larger than the other two, with a dorsal pharyngeal gland orifice at its base; right and left subventral sectors form a small cuticularized ridge. Telostegostom slightly cuticularized, connecting metastegostom and pharynx; ventral part a little deeper than the dorsal part. Anterior pharynx (pro- and metacorpus excluding stoma) a little longer than the posterior pharynx (isthmus and basal bulb). Procorpus muscular, slender, occupying ca. 40% to 50% of the corresponding body diameter. Metacorpus well developed, forming a muscular median bulb. Isthmus glandular, gradually increasing in width to a glandular basal bulb. Nerve ring surrounding the middle or slightly posterior part of the isthmus. Excretory pore located around the posterior end of the isthmus or anterior end of the basal bulb, perpendicular to body surface, and possess tube-like excretory–secretory duct. A large cell visible on the ventral side, at the level of or a little posterior to the cardia, assumed to be a secretory cell associated with the secretory–excretory system. Pharyngo–intestinal valve (cardia) well developed.

Male: Testis single, overlapping with the intestine ventrally and laterally on the right side of the intestine; anterior end reflexed dorsally or ventrally; the reflexed part occupying 7.5% to 22.1% of genital tract length. Spermatocytes arranged in multiple (2–3) rows in the reflexed part, then in a single row in the middle part with developed sperm tightly packed in the posterior part of the testis. *Vas deferens* tube-like, about 1/3 of the gonad in length, possessing glandular and thick walls, usually empty in cultured individuals. Intestine and *vas deferens* fused to form a narrow cloacal tube around the anterior end of the spicule. Three (two subventral and one dorsal) cloacal (rectum) gland cells visible around the anterior end of the cloacal tube. Spicules paired, separate; manubrium small, rounded, separated from the other parts of the spicule with weak constriction; calomus–lamina complex clearly bent at 1/3 of its length from the anterior end, posterior part smoothly narrowing to a bluntly pointed and ventrally curved tip. Gubernaculum ca. 1/2 of the spicule in length, possessing a rounded anterior part and a pointed distal end in lateral view; the distal 2/3 of the length attached to the dorsal side of the spicule and a membrane-like extension present at the part attached to the spicule, which covers (overlaps) the dorsal side of the spicule. Tail smoothly tapered and possessing a spike at the tail tip; spike conical, as long as or a little longer than half the cloacal body

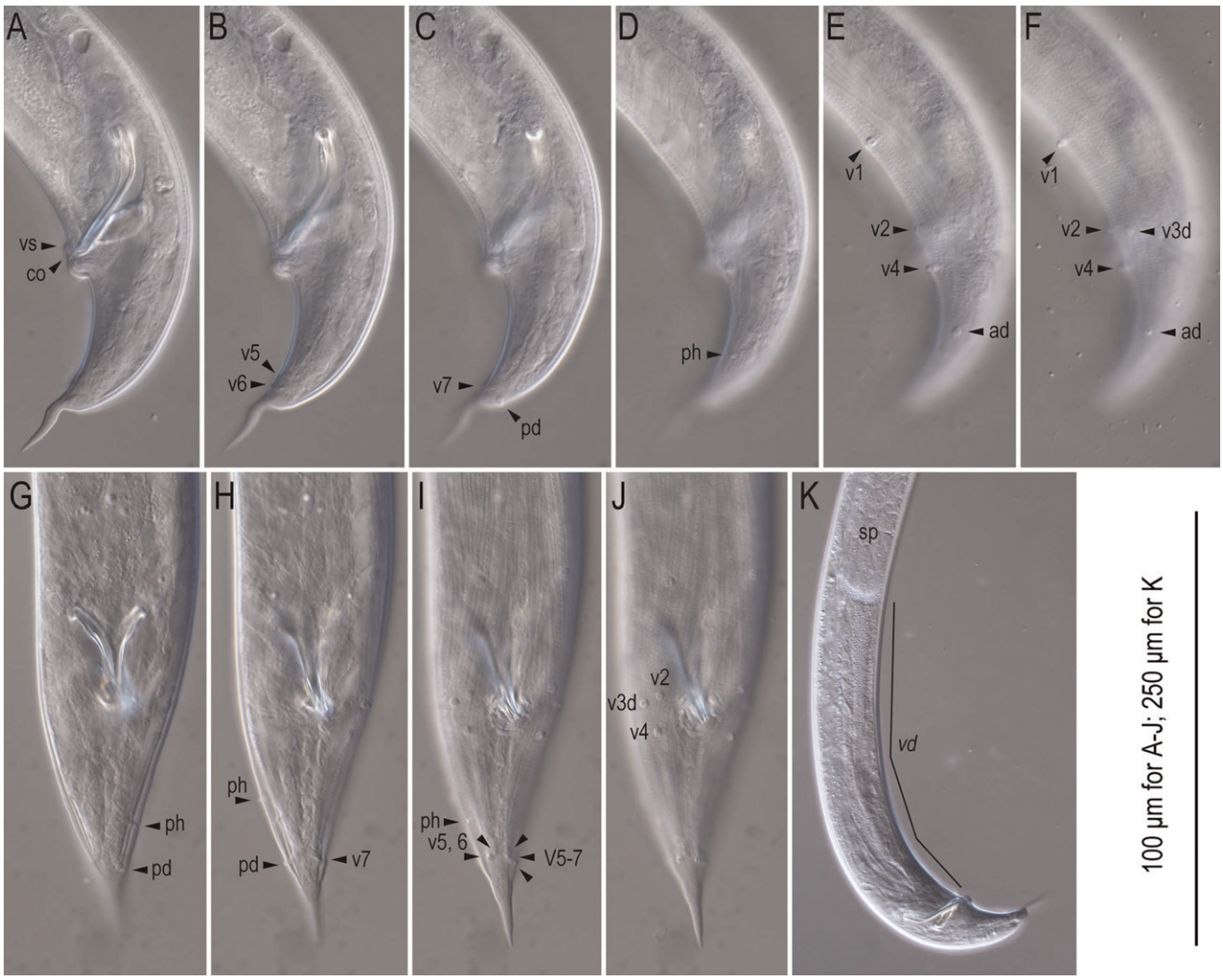

FIG. 5. Male tail region of *Diplogasteroides asiaticus* n. sp. in different focal planes. A–F. Left lateral view showing the cloacal opening (CO), genital papillae (v + number, ad, pd, vs), and phasmid (ph). G–H. Ventral view showing the CO, genital papillae (v + number, ad, pd), and phasmid (ph). K. Right lateral view showing packed sperm (sp) and *vas deferens* (vd).

diameter (CBD). Nine pairs of genital papillae and a papilla on the precloacal lip present. Bursa or bursal velum absent. First subventral pair (v1) at 1.5 CBD anterior to the cloacal opening (CO); second subventral (v2) and third lateral (v3d) pairs close to each other, located just (ca. 1/5 CBD) anterior to the CO; CO a short horizontal slit; fourth subventral pair (v4) just (ca. 1/5 CBD) posterior to the CO; fifth lateral pair (ad) around the midpoint between the CO to the root of the tail spike or located ca. 1 CBD posterior to the CO; sixth to eighth subventral pairs (v5–v7) close to each other, located just anterior to the root of the tail spike, v6 a little more ventral than v5 and v7; ninth dorsal pair (pd) on same level with v7. Phasmids laterally located, almost at the midpoint between ad and v5 or a little closer to ad. Within these papillae, v1-ad similar in size, v5 and v6 very small, difficult to observe, v7 and pd small, but larger than v5 and v6. v6 has a split tip and the appearance of a short, wide papilla with a flattened tip; the others are regular setiform papillae.

Female: Gonads paired. Anterior gonad to the right of the intestine, posterior gonad to the left of the intestine. The basic composition of the anterior and posterior gonads is identical and the anterior gonad is described here. The gonad is arranged from the ovary to vulva–vagina as ovary, ovary–oviduct junction tissue, oviduct, spermatheca, uterus, and vulva–vagina. Ovary reflexed along its entire length (=antidromous reflexion). Posterior (distal) tip sometimes reaches or exceeds the vulval position, i.e., sometimes anterior and posterior ovaries overlap around the vulval position. Oocytes arranged as multiple (2–5) rows in the distal 1/2 of the ovary, with well-developed oocytes arranged in a single row in the other half of the ovary. One or two of the most developed (largest) oocyte(s) located at the anterior end (closest to the oviduct) clearly darker than the other less-developed oocytes. Ovary and oviduct connected to a tissue constructed of small rounded cells. Oviduct tube-like, located between the ovary and spermatheca, constructed with long, column-like cells.

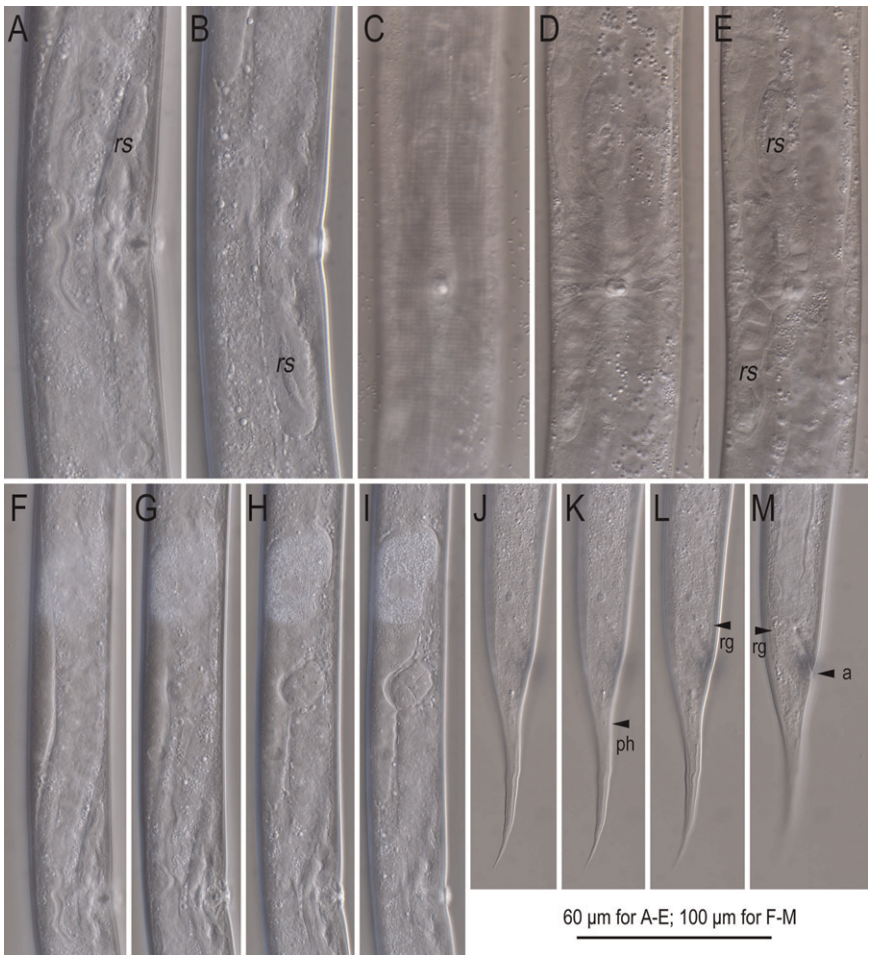

Fig. 6. Female gonad and tail region of *Diplogasteroides asiaticus* n. sp. in different focal planes. A, B. Right lateral view of the vulval region showing the *receptaculum seminis* (rs). C–E. Ventral view of the vulval region showing the *receptaculum seminis* (rs). F-I. Right lateral view of the entire anterior gonad. J–M. Right lateral view of the female tail showing the phasmid (ph), rectal glands (rg), and anal opening (a).

Spermatheca long, constructed with flat cells, whose surface has a polygonal tile-like pattern, sometimes filled with well-developed amoeboid sperm. Uterus ca. 1/2 of the spermatheca in length, constructed with rounded cells. Vagina perpendicular to the body surface, constricted with a sphincter muscle at the uterus–vulva junction. Vulva pore-like, rather flat and not protuberant in lateral view. Glue-like transparent copulatory plug can be observed around the vulva in mated females. Vulval glands present, but not observed clearly. In addition to the regular gonadal system, a pair of sacs (*receptaculum seminis*) present at the vulval region overlaps the uterus. The thick wall of the *receptaculum seminis* is clearly observed when it is empty and becomes less visible when it contains many sperm. Anterior and posterior sacs on the left and right of the intestine, respectively, i.e., opposite sides of the uterus, i.e., uteri and *receptaculum seminis* forming X shape in ventral view. The sacs sometimes contain a "pouch of sperm," constructed of ca. 20 sperm cells, and form an elongated oval shape. Rectum ca. one anal body diameter in length, separated from the intestine by a sphincter muscle. Three (two subventral and one dorsal) anal (rectum) glands clearly visible at the intestine–rectum junction. Anus a dome-shaped slit in ventral view; posterior anal lip a little protuberant in lateral view. Small oval-shaped phasmid clearly visible laterally ca. 1.5 anal body diameters posterior to the anal opening. Tail elongated, conical, smoothly tapering to a finely pointed tip.

Diagnosis and relationships: Diplogasteroides asiaticus n. sp. is characterized by its stomatal morphology, a tube-like stoma with three small rod-like dorsal teeth and two subventral ridges; a spicule that is ventrally bent 1/3 from the anterior end; a gubernaculum with an inverted water droplet-shape in lateral view; nine pairs of genital papillae with an arrangement of <v1, (v2, v3d), C, v4, ad, ph, (v5, v6, v7), pd>, which is equivalent to <P1, (P2, P3d), C, P4, P5d, ph, (P6, P7, P8), P9d> in Kanzaki et al. (2013); a short tail spike about half the length of the diameter of the cloacal body in males; a well-developed sac-like *receptaculum seminis* at the vulval position in females. In addition to the morphological characters, which are common to several species in the genus, the new species can be characterized by its

TABLE 1. Morphometrics of *Diplogasteroides asiaticus* n. sp. Values were measured using temporarily water-mounted materials except for the holotype male. All measurements are in μm and in the form: mean ± SD (range).

	Holotype male	Males in temporary water mount	Females in temporary water mount
n	–	15	15
Body length (L)	773	722 ± 56 (653–834)	858 ± 40 (771–931)
a	27.0	27.7 ± 1.7 (25.3–30.5)	24.0 ± 1.6 (22.2–27.9)
b	6.0	5.5 ± 0.4 (4.5–6.0)	6.3 ± 0.3 (5.5–7.0)
c	14.4	12.8 ± 0.9 (11.2–14.0)	9.8 ± 0.4 (9.0–10.7)
c'	2.2	2.3 ± 0.2 (2.0–2.6)	4.2 ± 0.3 (3.8–4.7)
T[a] or V	74.8	62.9 ± 4.4 (56.0–72.9)	52.2 ± 0.7 (51.1–53.4)
Maximum body diam.	29	26 ± 1.3 (24–29)	36 ± 2.1 (31–39)
Stoma width	4.2	3.8 ± 0.3 (3.4–4.3)	4.0 ± 0.4 (3.4–4.6)
Stoma depth	11.2	11.8 ± 0.6 (10.9–13.1)	12.2 ± 0.6 (10.9–13.1)
Stoma depth/width ratio	2.7	3.1 ± 0.3 (2.7–3.7)	3.1 ± 0.4 (2.5–3.7)
Anterior pharynx length	66	63 ± 3.2 (57–70)	66 ± 3.2 (63–74)
Posterior pharynx length	57	57 ± 3.5 (50–64)	63 ± 4.5 (51–70)
Anterior/posterior pharynx ratio	1.17	1.09 ± 0.04 (1.02–1.15)	1.14 ± 0.06 (1.07–1.28)
Median bulb diam.	13.8	15.1 ± 0.9 (13.7–17.1)	17.4 ± 1.1 (15.4–20.0)
Basal bulb diam.	11.9	13 ± 1.0 (11.4–14.9)	15.2 ± 1.1 (13.1–17.1)
Nerve ring from anterior end	92	92 ± 3.9 (84-100)	98 ± 4.0 (91-107)
Nerve ring from the posterior end of median bulb	19.6	18.3 ± 1.6 (14.3–20.0)	19.4 ± 1.9 (17.1–22.9)
Excretory pore from anterior end	112	114 ± 8.0 (104–129)	120 ± 8.1 (97–134)
Excretory pore from the posterior end of median bulb	39	40 ± 6.9 (31–59)	41 ± 7.9 (16–49)
Testis length[b]	371	300 ± 36 (226–356)	–
Testis reflection[c]	85	73 ± 19 (34–106)	–
Vas deferens length	206	154 ± 22 (119–194)	–
Vas deferens/total gonad length in %	35.7	34.0 ± 4.4 (25.2–40.5)	–
Vulval body diam.	–	–	34 ± 2.0 (31–37)
Anterior ovary length	–	–	126 ± 18 (100–150)
Posterior ovary length	–	–	88 ± 21 (66–141)
Anterior/posterior ovary ratio	–	–	1.48 ± 0.3 (1.01–2.06)
Receptacle seminis length	–	–	112 ± 14 (96–149)
Anterior part of *receptacle seminis*	–	–	54 ± 8.1 (43–76)
Posterior part of *receptacle seminis*	–	–	59 ± 7.5 (49–73)
Anterior/posterior *receptacle seminis* ratio	–	–	0.92 ± 0.10 (0.73–1.06)
Cloacal or anal body diam	24	24 ± 0.7 (23–26)	21.1 ± 1.1 (18.9–22.9)
Tail length	54	57 ± 4.1 (49–62)	88 ± 4.9 (77–99)
Tail spike length	17.5	17.3 ± 2.4 (12.6–21.1)	–
Tail spike/total tail length in %	32.5	30.5 ± 2.5 (25.9–35.2)	–
Spicule length (curve)	33	30 ± 1.5 (27–32)	–
Spicule length (chord)	29	27 ± 1.5 (24–29)	–
Gubernaculum length	19.6	17.1 ± 1.0 (16.0–19.4)	–
Major axis of sperm in spermatheca	–	–	10.3 ± 1.5 (7.6–11.8)
Minor axis of sperm in spermatheca	–	–	7.3 ± 0.3 (5.6–9.0)
Major/minor axis ratio of sperm in spermatheca	–	–	1.4 ± 0.3 (1.0–2.0)
Major axis of egg	–	–	65 ± 4.2 (55–70)
Minor axis of egg	–	–	28 ± 2.2 (24–32)
Major/minor axis ratio of egg	–	–	2.4 ± 0.2 (1.9–2.8)

[a] Calculated including *vas deferens* length, i.e., 100 × (testis + *vas deferens*)/body length.
[b] Excluding *vas deferens*.
[c] Reflexed part is included in the total testis length.

molecular sequences of near-full-SSU and D2-D3 LSU as the species-specific molecular profile.

As suggested by Sudhaus and Fürst von Lieven (2003), the genus contains morphologically variable species (e.g., species with single or paired female gonad [s]). Thus, as in a previous study (Kanzaki et al., 2013), we employed the typological characters suggested by Andrássy (1984) to identify typologically similar species.

The new species, *D. asiaticus* n. sp., is typologically close to *D. adephagus* (Massey, 1974) Sudhaus and Fürst von Lieven, 2003, *D. andrassyi*, *D. carinthiacus* (Fuchs, 1931) Rühm in Körner, 1954, *D. frontali* (Massey, 1974) Sudhaus and Fürst von Lieven, 2003, *D. haslacheri* (Fuchs, 1931) Rühm in Körner, 1954, and *D. janae* Massey, 1962. The new species and the above six species share paired gonads in females, a water droplet-shaped male gubernaculum, a spicule ventrally bent at 1/2 to 1/3 of the spicule length from the manubrium, and a biological character: association with wood-boring scolytid or cerambycid beetles (Rühm, 1956; Massey, 1974; Sudhaus and Fürst

von Lieven, 2003; Kanzaki et al., 2013). Within these species, *D. adephagus*, *D. frontali*, and *D. janae* were described as having five, six, or seven pairs of genital papillae (summarized in Massey, 1974). As suggested in previous studies (Sudhaus and Fürst von Lieven, 2003; Kanzaki et al., 2013), these numbers of papillae are unusual and several pairs may have been missed during observations using light microscopy. Thus, we examined the positions of the v1 and v2 papillae, which appeared to be drawn correctly. Other questionable characters and quantitative characters were not used in the comparison.

Within these six species, *D. asiaticus* n. sp. is distinguished from the three American species by the position of the male v2 genital papillae. The v2 papillae in all three American species, *D. adephagus*, *D. frontali*, and *D. janae*, are located midway between v1 and the CO or closer to v1 (Massey, 1962, 1974), while the v2 of the new species and the other three species, *D. andrassyi*, *D. carinthiacus*, and *D. haslacheri*, is obviously closer to the CO than to v1 (Fuchs, 1931; Rühm, 1956; Kanzaki et al., 2013).

Based on the drawings and live materials (Fuchs, 1931; Rühm, 1956; Kanzaki et al., 2013), *D. asiaticus* n. sp., *D. andrassyi*, *D. carinthiacus*, and *D. haslacheri* are almost identical in typological characters, i.e., these four species share the arrangement of genital papillae and phasmids as described above and have an elongated, conical female tail. These species can be distinguished by the relative length of the male tail spike, the position of excretory pore and the position of nerve ring.

However, *D. asiaticus* n. sp. is distinguished from *D. andrassyi* by the relative length of male tail spike, shorter than CBD vs. longer than CBD (Kanzaki et al., 2013); from *D. carinthiacus* by the position of nerve ring, around the middle or a little posterior part of isthmus vs. at the posterior part of isthmus, and the relative length of male tail spike, shorter thanCBD vs. longer than or almost the same as CBD (Fuchs, 1931; Rühm, 1956)from *D. haslacheri* by the excretory pore position, at the level of basal bulb or cardia vs. around the middle of isthmus, and female tail morphology, i.e., although both species have a slightly elongated conical tail, the tail of *D. haslacheri* is a little more slender than the new species. This character can be represented by the phasmid position in females being ca. 1.5 vs. ca. 2 ABD posterior to the anus (Fuchs, 1931; Rühm, 1956).

Molecular barcodes and phylogeny: The molecular sequences of the SSU, D2-D3 LSU and mtCOI from the new species are deposited in the GenBank database with the accession numbers LC027672, LC027673, and LC027676, respectively.

The BLAST homology search revealed that the new species is molecularly very close to *D. andrassyi* and there is only one base pair difference in SSU and seven base pair differences in D2-D3 LSU.

The molecular phylogenetic status of *D. asiaticus* n. sp. inferred from Bayesian analysis suggested that the new species forms a well-supported clade with *D. andrassyi* (Fig. 7).

Hybridization test: Morphologically cryptic species are common in nematodes and hybridization tests can be utilized to define biological species (Kanzaki et al., 2012b; Félix et al., 2014). To this end, such tests were performed between *D. andrassyi* and *D. asiaticus* n. sp. Crosses were assayed for the presence of embryo production and F_1 viability. Further crosses between F_1 siblings were performed to ascertain F_2 viability, which delineates some cryptic nematode species (Dey et al., 2012).

All conspecific crosses of *D. andrassyi* (n = 10 crosses) and *D. asiaticus* n. sp. (n = 8) yielded viable F_1 and F_2 adults (Table 2). In addition, all conspecific F_1 sibling crosses of *D. andrassyi* (n = 2) and *D. asiaticus* n. sp. (n = 2) yielded viable F_2 adults (Table 3). However, reciprocal heterospecific crosses revealed asymmetries in hybrid fitness (Table 2). Whereas all crosses of *D. asiaticus* n. sp. females and *D. andrassyi* males (n = 12) generated viable F_1 adults, only half of the reciprocal crosses utilizing *D. andrassyi* females and *D. asiaticus* n. sp. males generated viable F_1 adults (8 out of 15 crosses). In addition, many crosses between *D. andrassyi* females and *D. asiaticus* n. sp. males did not generate F_1 embryos (7 out of 15 crosses). As mating behavior was observed in both crossing directions, this particular hybridization asymmetry is likely the result of gametic (as opposed to postzygotic) isolation. Furthermore, in all of these hybrid crosses, no viable F_2 adults were observed. To examine this further, additional crosses between hybrid F_1 adults were performed (Table 3). In all hybrid F_1 crosses (n = 5 for F_1 sibling crosses derived from *D. andrassyi* females and *D. asiaticus* n. sp. males; n = 2 for F_1 sibling crosses derived from *D. asiaticus* n. sp. females and *D. andrassyi* males), no viable F_2 adults were observed. For F_1 sibling crosses derived from *D. asiaticus* n. sp. females and *D. andrassyi* males, no embryos were observed. For F_1 sibling crosses derived from *D. andrassyi* females and *D. asiaticus* n. sp. males, embryos were observed in a fraction (3/5) of crosses. All of these embryos arrested during embryogenesis. Thus, the inability of *D. andrassyi* and *D. asiaticus* n. sp. to produce viable F_2 progeny indicates that they are distinct biological species.

Type locality, carrier insect, and habitat: Dauer (dispersal third stage) juveniles of *D. asiaticus* n. sp. were isolated from male genitalia or female ovipositors of *M. alternatus*. The beetles emerged from a dead *P. densiflora* log in June 2013. The log was collected at FFPRI in April 2013.

Type materials: A holotype male, nine paratype males, and 10 paratype females were deposited in the U.S. Department of Agriculture (USDA) Nematode Collection, Beltsville, MD, with the the U.S. Department of Agriculture Nematode Collection (USDANC) collection numbers *Diplogasteroides asiaticus* T-681t (holotype male),

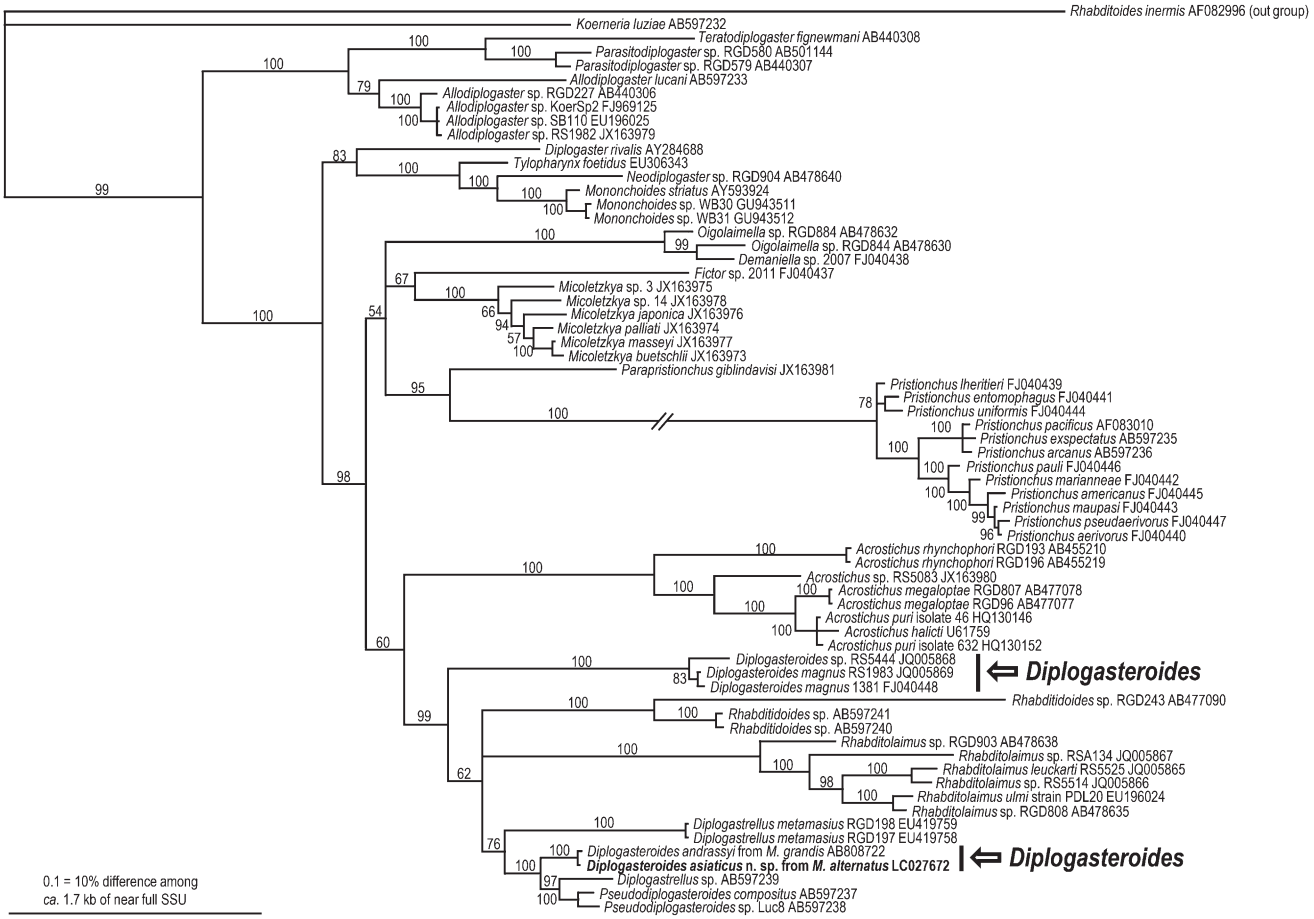

FIG. 7. Molecular phylogenetic status of *Diplogasteroides asiaticus* n. sp. The Bayesian tree was inferred from the nearly full-length SSU under the GTR + I + G model (lnL = 15494.3906; freqA = 0.2361; freqC = 0.2137; freqG = 0.27; freqT = 0.2801; R(a) = 1.223; R(b) = 3.0468; R(c) = 2.541; R(d) = 0.4479; R(e) = 5.3816; R(f) = 1; Pinva = 0.423; Shape = 0.5793). Posterior probability values exceeding 50% are given for appropriate clades.

T-6445p-T-6453p (paratype males) and T-6454p- T-6463p (paratype femeles), and five paratype males and five paratype females were deposited in the Forest Pathology Laboratory Collection, FFPRI with collection numbers *Diplogasteroides asiaticus* PM01-05 (paratype males) and PF01-05 (paratype females). Several more unmounted specimens in dehydrated glycerin are available from the FFPRI collection (N. Kanzaki) upon request.

Etymology: The species epithet, *asiaticus*, is derived from its type locality, East Asia.

Life cycle: Because dauer (third-stage dispersal) juveniles of *D. asiaticus* n. sp. were isolated from genitalia and ovipositors of *M. alternatus* and propagated on an *E. coli* lawn, the nematode is considered to be a bacteria-feeding species phoretically associated with the beetle, i.e., typical life history of the genus *Diplogasteroides* (e.g., Sudhaus and Fürst von Lieven, 2003).

DISCUSSION

Additional remarks on morphological characters: In a previous study (Kanzaki et al., 2013), the authors confirmed the presence of a large *receptaculum seminis* and morphologically modified v6 genital papillae in

TABLE 2. Experimental design and results of hybridization test.

Cross	F_1 embryos[a]	Viable F_1 adults[a]	Viable F_2 adults[a]
Diplogasteroides asiaticus ♀ × *D. asiaticus* ♂	10/10	10/10	10/10
Diplogasteroides. andrassyi ♀ × *D. andrassyi* ♂	8/8	8/8	8/8
D. asiaticus ♀ × *D. andrassyi* ♂	12/12	12/12	0/12
D. andrassyi ♀ × *D. asiaticus* ♂	8/15	8/15	0/15

[a] Fraction of crosses that produced these.

TABLE 3. Experimental design and results of additional F1 intercrosses.

Parental cross[a]	F_2 embryos[b]	Viable F_2 adults[b]
Diplogasteroides asiaticus ♀ × *D. asiaticus* ♂	2/2	2/2
Diplogasteroides andrassyi ♀ × *D. andrassyi* ♂	2/2	2/2
D. asiaticus ♀ × *D. andrassyi* ♂	0/2	0/2
D. andrassyi ♀ × *D. asiaticus* ♂	3/5	0/5

[a] The parental cross that generated the animals for the subsequent F1 intercrosses.

[b] Fraction of F1 intercrosses that produced these.

D. andrassyi, a close relative of *D. asiaticus* n. sp. Furthermore, several species in different phylogenetic clades, e.g., *D. magnus* clade and *Pseudodiplogasteroides* spp., have similar characters. *D. magnus* clade has a small, but distinctive oval-shaped *receptaculum seminis* at the level of vulval opening (Kiontke et al., 2001), and *Pseudodiplogasteroides* spp. have a long and distinctive *receptaculum seminis*, which is very similar to that of *D. andrassyi* (Kanzaki et al., 2013; Kanzaki, unpubl. observation). The characters were also confirmed in the new species. Because these characters are not found in *Diplogastrellus* and *Rhabditolaimus*, which belong to the same clade with *Diplogasteroides* and *Pseudodiplogasteroides* Körner, 1954 (Fig. 7), these characters are assumed to have arisen independently in these clades and are shared within each clade. Re-isolation and close examination of previously described *Diplogasteroides* spp. followed by detailed morphological observation and molecular sequencing are necessary to characterize this phylogenetic group.

Remarks on molecular sequence differences and hybridization: The molecular SSU and D2-D3 LSU sequences from the new species are very close to those of *D. andrassyi*. The difference level, one base pair in ca. 1.7 kbs in the SSU and seven base pairs in ca. 0.7 kbs in the D2-D3 LSU, is almost the same as for intraspecific differences in other groups of nematodes. For example, aphelenchid insect associates *Bursaphelenchus* spp. have ca. 15 bps to 20 bps of intraspecific variation in D2-D3 and 1- to 2-bp variation in the SSU (e.g., Kanzaki et al., 2012a; Kanzaki and Akiba, 2014). Even *Pristionchus pacificus* and *Pristionchus exspectatus*, one of the closest sister species pairs of diplogastrids, have 10-bp differences in the SSU and 24-bp differences in ca. 1.2 kbs of the D1-D4 LSU (Kanzaki et al., 2012b). The distribution range of *D. asiaticus* n. sp. and its close relative *D. andrassyi* almost overlap each other, i.e., both are associated with *Monochamus* beetles and Pinaceae conifers in Japan, and the speciation is assumed to have occurred sympatrically. However, at present, we do not have sufficient information on the mechanism of their speciation. Detailed comparison of these two species may provide important information on sympatric speciation.

Literature Cited

Andrássy, I. 1984. Klasse Nematoda (Ordnungen Monhysterida, Desmoscolecida, Araeolaimida, Chromadorida, Rhabditida). Stuttgart, Germany: Gustav Fischer Verlag.

de Man, J. G. 1912. Helminthologische Beiträge. Zoologische Jahrbücher (Systematik), Suppl. 15:439–464.

Dey, A., Jeon, Y., Wang, G. X., and Cutter, A. D. 2012. Global population genetic structure of *Caenorhabditis remanei* reveals incipient speciation. Genetics 191:1257–1269.

Félix, M. A., Braendle, C., and Cutter, A. D. A. 2014. Streamlined system for species diagnosis in *Caenorhabditis* (Nematoda: Rhabditidae) with name designations for 15 distinct biological species. PLoS ONE 9:e94723.

Fuchs, G. 1931. Die Genera: 1. *Rhabditolaimus* Fuchs, 2. *Neodiplogaster* Cobb, 3. *Tylenchodon* Fuchs. Zentralblatt für das gesamte Forstwesen 57:177–194.

Hooper, D. J. 1986. Handling, fixing, staining and mounting nematodes. Pp. 59–80 *in* J.F. Southey, ed. Methods for work with plant and soil nematodes. London: Her Majesty's Stationary Office.

Huelsenbeck, J. P., and Ronquist, F. 2001. MR BAYES: Bayesian inference of phylogenetic trees. Bioinformatics 17:1754–1755.

Kanzaki, N. 2013. Simple methods for morphological observation of nematodes. Nematological Research 43:9–13.

Kanzaki, N., and Akiba, M. 2014. Isolation of *Bursaphelenchus mucronatus kolymensis* from *Monochamus nitens* from Japan. Nematology 16:743–745.

Kanzaki, N., and Futai, K. 2002. A PCR primer set for determination of phylogenetic relationships of *Bursaphelenchus* species within *xylophilus* group. Nematology 4:35–41.

Kanzaki, N., and Giblin-Davis, R. M. 2015. Diplogastrid systematics and phylogeny. Pp. 43–76 *in* R. J. Sommer, ed. Nematology monographs and perspectives, vol. 11, *Pristionchus pacificus*—a nematode model for comparative and evolutionary biology. Leiden: Brill.

Kanzaki, N., Maehara, N., Aikawa, T., and Matsumoto, K. 2012a. *Bursaphelenchus firmae* n. sp. isolated from *Monochamus grandis* (Coleoptera: Cerambycidae) isolated from *Abies firma* Sieb. Zucc. Nematology 14:395–404.

Kanzaki, N., Ragsdale, E. J., Herrmann, M., Mayer, W. E., and Sommer, R. J. 2012b. Description of three *Pristionchus* species (Nematoda: Diplogastridae) from Japan that form a cryptic species complex with the model organism *P. pacificus*. Zoological Science 29:403–417.

Kanzaki, N., Tanaka, R., Hirooka, Y., and Maehara, N. 2013. Description of *Diplogasteroides andrassyi* n. sp., associated with *Monochamus grandis* and Pinaceae trees in Japan. Journal of Nematode Morphology and Systematics 16:35–47.

Katoh, K., Misawa, K., Kuma, K., and Miyata, T. 2002. MAFFT: a novel method for rapid multiple sequence alignment based on fast Fourier transform. Nucleic Acids Research 30:3059–3066.

Kikuchi, T., Aikawa, T., Oeda, Y., Karim, N., and Kanzaki, N. 2009. A rapid and precise diagnostic method for detecting the pinewood nematode *Bursaphelenchus xylophilus* by loop-mediated isothermal amplification (LAMP). Phytopathology 99:1365–1369.

Kiontke, K., Manegold, A., and Sudhaus, W. 2001. Redescription of *Diplogasteroides nasuensis* Takaki, 1941 and *D. magnus* Völk, 1950 (Nematoda: Diplogastrina) associated with Scarabaeidae (Coleoptera). Nematology 3:817–832.

Körner, H. 1954. Die Nematodenfauna des vergehenden Holzes und ihre Beziehungen zu den Insekten. Zoologische Jahrbücher (Systematik) 82:245–353.

Larget, B., and Simon, D. L. 1999. Markov chain Monte Carlo algorithms for the Bayesian analysis of phylogenetic trees. Molecular Biology and Evolution 16:750–759.

Massey, C. L. 1962. New species of Diplogasteridae (Nematoda) associated with bark beetles in the United States. Proceedings of the Helminthological Society of Washington 29:67–75.

Massey, C. L. 1974. Biology and taxonomy of nematode parasites and associates of bark beetles in the United States. Agriculture Handbook no. 446, Washington, DC: USDA Forest Service.

Micoletzky, H. 1922. Die freilebenden Erd-Nematoden. Archiv für Naturgeschichte. Abteiliung A 87:1–650.

Minagawa, N., and Mizukubo, T. 1994. A simplified procedure of transferring nematodes to glycerol for permanent mounts. Japanese Journal of Nematology 24:75.

Posada, D., and Crandall, K. A. 1998. Modeltest: testing the model of DNA substitution. Bioinformatics 14:817–818.

Rühm, W. 1956. Die Nematoden der Ipiden. Parasitologische Schriftenreihe 6:1–437.

Sudhaus, W., and Fürst von Lieven, A. 2003. A phylogenetic classification and catalogue of the Diplogastridae (Secernentea, Nematoda). Journal of Nematode Morphology and Systematics 6:43–89.

Susoy, V., Ragsdale, E. J., Kanzaki, N., and Sommer, R. J. 2015. Rapid diversification associated with a macroevolutionary pulse of developmental plasticity. eLife: in press.

Tanaka, R., Kikuchi, T., Aikawa, T., and Kanzaki, N. 2012. Simple and quick methods for nematode DNA preparation. Applied Entomology and Zoology 47:291–294.

Wood, W. B. 1988. The Nematode *Caenorhabditis elegans*. Cold Spring Harbor, NY: Cold Spring Habor Laboratory Press.

Völk, J. 1950. Die Nematoden der Regenwürmer und aasbesuchenden Käfer. Zoologische Jahrbücher (Systematik) 79:1–70.

Ye, W., Giblin-Davis, R. M., Braasch, H., Morris, K., and Thomas, W. K. Phylogenetic relationships among *Bursaphelenchus* species (Nematoda: Parasitaphelenchidae) inferred from nuclear ribosomal and mitochondrial DNA sequence data. Molecular Phylogenetics and Evolution 43:1185–1197.